

# Electronic Structure of $\text{KFe}_2\text{Se}_2$ from First-Principles Calculations

Chao Cao<sup>1</sup> and Jianhui Dai<sup>1,2</sup>

<sup>1</sup>*Condensed Matter Physics Group, Department of Physics,  
Hangzhou Normal University, Hangzhou 310036, China*

<sup>2</sup>*Zhejiang Institute of Modern Physics, Department of Physics, Zhejiang University, Hangzhou 310027, China*

(Dated: October 29, 2018)

Electronic structure and magnetic properties for iron-selenide  $\text{KFe}_2\text{Se}_2$  are studied by first-principles calculations. The ground state is collinear antiferromagnetic with calculated  $2.26 \mu_B$  magnetic moment on Fe atoms; and the  $J_1, J_2$  coupling strengths are calculated to be 0.038 eV and 0.029 eV. The states around  $E_F$  are dominated by the Fe-3d orbitals which hybridize noticeably to the Se-4p orbitals. While the band structure of  $\text{KFe}_2\text{Se}_2$  is similar to a heavily electron-doped  $\text{BaFe}_2\text{As}_2$  or FeSe system, the Fermi surface of  $\text{KFe}_2\text{Se}_2$  is much closer to FeSe system since the electron sheets around  $M$  is symmetric with respect to  $x$ - $y$  exchange. These features, as well as the absence of Fermi surface nesting, suggest that the parent  $\text{KFe}_2\text{Se}_2$  could be regarded as an electron doped 11 system with possible local moment magnetism.

PACS numbers: 74.70.-b, 74.25.Ha, 74.25.Jb, 74.25.Kc

The discovery of iron-based compounds, typically represented by  $\text{LaFeAsO}^1$  (1111-type),  $\text{BaFe}_2\text{As}_2^2$  (122-type) and  $\text{FeSe}^{3,4}$  (11-type), has triggered enormous enthusiasm in searching for the new high transition temperature superconductors without copper<sup>5-9</sup>. Ever since the discovery, density functional studies have been performed to explore the electronic structure and the pairing mechanism of the system. Calculations have been performed on  $\text{LaFeAsO}^{10-16}$ , and the ground state is found to be a collinear anti-ferromagnetism (COL) state. The magnetic ordering was proposed to be the consequence of the Fermi surface nesting phenomena<sup>10,11,13</sup>, which is also present in the  $\text{BaFe}_2\text{As}_2$  parent compound<sup>17</sup>. The Fermi surface nesting is thus considered closely related with the superconducting (SC) phenomena since it is suppressed in SC phase. On the other hand, the  $J_1$ - $J_2$  Heisenberg model based on a local moment picture<sup>12,16,18</sup> was also proposed to account for the magnetic structure. It is also found that the band energy dispersion of these compounds should be calculated using the unrelaxed experimental structure in order to compare with the experiments<sup>19,20</sup>, and that the ordered magnetic moments on Fe atom are systematically overestimated in density functional calculations.

Recently, another substance with similar chemical composition,  $\text{KFe}_2\text{Se}_2$ , has been produced<sup>21</sup>. The material is reported to be iso-structural to  $\text{BaFe}_2\text{As}_2$ , and the superconductivity as high as 30 K is reported when it is intrinsically doped ( $\text{K}_{1-x}\text{Fe}_2\text{Se}_2$  with  $x = 0.2$ ). Question thus arises that whether this material represents a new family or it is one of the discovered class. More specifically, since  $\text{KFe}_2\text{Se}_2$  is structurally close to  $\text{BaFe}_2\text{As}_2$  but chemically close to FeSe, it is interesting to clarify which one is closer to its electronic structure.

In this paper, we report our first-principles study of this compound. We demonstrate that the electronic structure of the parent  $\text{KFe}_2\text{Se}_2$  could be regarded as an electron doped 11 system, instead of the structurally much closer  $\text{BaFe}_2\text{As}_2$ . All the calculations were per-

formed with the QUANTUM ESPRESSO code<sup>22</sup>, while an accurate set of PAW data<sup>23</sup> were employed throughout the calculation. A 48 Ry energy cut-off ensures the calculations converge to 0.1 mRy, and all structures were optimized until forces on individual atoms were smaller than 0.1 mRy/bohr and external pressure less than 0.5 kbar. For non-magnetic (NM) and checkerboard antiferromagnetic (CBD) states, a  $8 \times 8 \times 8$  Monkhorst-Pack k-grid<sup>24</sup> was found to be sufficient; while for the collinear anti-ferromagnetic (COL) state and bi-collinear anti-ferromagnetic (BIC) state,  $6 \times 6 \times 8$  and  $16 \times 8 \times 4$  Monkhorst-Pack k-grid were needed to ensure the convergence to  $< 1$  meV/Fe, respectively. The PBE flavor of general gradient approximation (GGA) to the exchange-correlation functional<sup>25</sup> was applied throughout the calculations.

We first examine several possible spin configurations for  $\text{KFe}_2\text{Se}_2$  (TABLE I). The column expt indicates calculation with experimental structure and non-magnetic spin configuration, while the structures are fully optimized (lattice constants as well as internal coordinates) for NM/CBD/COL/BIC columns. It is therefore apparent that the collinear phase, which is 57 meV/Fe lower than the NM phase, is the ground state of  $\text{KFe}_2\text{Se}_2$ . This magnetic state ordering was also double-checked with full-potential linearized augmented plane wave (FLAPW) method using the elk code<sup>26</sup>. A body-centered tetragonal (bct) to base-centered orthorhombic (bco) phase transition is also present in the process, although the orthorhombicity  $\epsilon = 1 - b/a = 0.03\%$  is almost negligible. Although the phase transition is not yet observed in the experiments, the resistivity measurement shows an abrupt change around  $T = 100\text{K}^{21}$ , which we propose to be due to the bco-bct phase transition. The magnetic moment on Fe atoms turns out to be  $2.26 \mu_B/\text{Fe}$  for the collinear phase, which is similar to those obtained in PAW calculations for  $\text{BaFe}_2\text{As}_2^{23}$ . In order to estimate the magnetic coupling strength, we incorpo-

rate the  $J_1$ - $J_2$  Heisenberg model, defined by

$$H = J_1 \sum_{\langle i,j \rangle} \vec{S}_i \cdot \vec{S}_j + J_2 \sum_{\langle\langle i,j \rangle\rangle} \vec{S}_i \cdot \vec{S}_j.$$

Where,  $\vec{S}_i$  is the spin operator (of magnitude  $S$ ) at the site  $i$ ,  $\langle i,j \rangle$  and  $\langle\langle i,j \rangle\rangle$  denote the summation over the nearest neighbor and the next nearest neighbor sites,  $J_1$  and  $J_2$  are the nearest neighbor and the next nearest neighbor exchange interactions, respectively. By calculating the total energy per Fe atom for the CBD and COL states and assuming  $S = 1$ , we obtain  $J_2 = 29$  meV and  $J_1 = 38$  meV, respectively.

TABLE I. Geometry, energetic and magnetic properties of  $\text{KFe}_2\text{Se}_2$ . Results in column expt were obtained using the experimental structure and spin-unpolarized calculations; while the NM/CBD/COL/BIC columns correspond to non-magnetic/checkerboard AFM/collinear AFM/bicollinear AFM configurations using the fully optimized structures (lattice constants as well as internal coordinates), respectively.  $E_\Delta$  is the total energy difference per iron atom referenced to the fully optimized NM structure, and  $m_{\text{Fe}}$  is the local magnetic moment on Fe.

	expt	NM	CBD	COL	BIC
a (Å)	3.9136	3.8791	3.9058	5.5930	3.8271
b (Å)	3.9136	3.8791	3.9058	5.5916	7.9530
c (Å)	14.0367	13.4476	13.6849	13.8525	14.4783
$E_\Delta$ (meV/Fe)	272	0	-18	<b>-57</b>	-39
$m_{\text{Fe}}$ ( $\mu_B$ )	0.0	0.0	1.49	2.26	2.58

Calculations with  $\text{LaFeAsO}$ ,  $\text{BaFe}_2\text{As}_2$ , and  $\text{FeSe}$  systems suggest that the band dispersions and DOS of these systems should be studied without structural optimization in order to compare with the experiments<sup>11,13,14,17,27-29</sup>; although their energetic properties as well as magnetism should be explored with structural relaxation. We followed this procedure, and the discussion in the rest of this paper will primarily focus on the calculations with unrelaxed (experimental) structure unless we explicitly specify. Firstly, we present the density of states (DOS), as well as the projected density of states (PDOS) calculations (FIG. 1). The DOS and PDOS of  $\text{KFe}_2\text{Se}_2$  resemble those of  $\text{BaFe}_2\text{As}_2$  systems, and exhibit typical characteristics of the layered structure. The contribution from Fe-3d and Se-4p orbitals dominates the states from  $E_F - 6.0$  eV to  $E_F + 2.0$  eV, while most of the K-4s contribution locates from  $E_F + 2.0$  eV to  $E_F + 6.0$  eV. A closer examination of the PDOS data shows that over 90% of the states from  $E_F - 2.0$  eV to  $E_F$  are from the Fe-3d orbitals, and that the Fe-3d/Se-4p orbital hybridizes considerably from  $E_F - 6.0$  eV to  $E_F - 3.2$  eV and from  $E_F$  to  $E_F + 2.0$  eV.

We further calculated the band structure for  $\text{KFe}_2\text{Se}_2$ , as shown in FIG. 2. Since the Se atom ( $4s^2 4p^4$ ) outermost shell has 1 more electron than the As atom ( $4s^2 4p^3$ ), the FeSe layer could be regarded as highly electron-doped. In fact, the band structure of  $\text{KFe}_2\text{Se}_2$  shows that

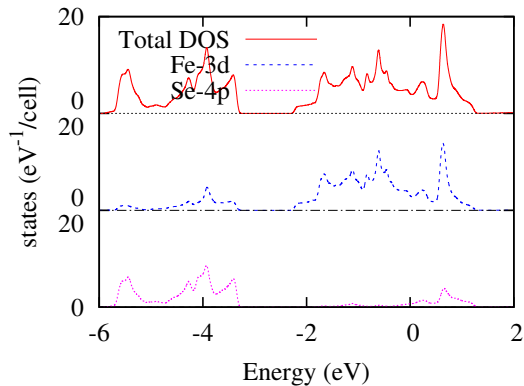


FIG. 1. Total and projected density of states of  $\text{KFe}_2\text{Se}_2$ . The upper panel (solid line) is the total DOS; middle panel (dashed line) is the PDOS on Fe-3d orbitals; lower panel (dotted line) is the PDOS on Se-4p orbitals. We show only the energy range from  $E_F - 6.0$  eV to  $E_F + 2.0$  eV.

the Fe- $3d_{zx(y)}$  and Fe- $3d_{x^2-y^2}$  bands are fully occupied, whereas these bands were the origin of the hole pockets in the  $\text{BaFe}_2\text{As}_2$  systems. At  $\Gamma$ , the  $3d_{zx}$  and  $3d_{zy}$  bands become degenerate due to the crystal symmetry. We define the energy difference between these two bands and the Fermi level at  $\Gamma$  to be  $\epsilon_t = E_F - \epsilon_\Gamma^{zx(y)}$ , and the difference between these two bands and the  $3d_{x^2-y^2}$  band at  $\Gamma$  to be  $\Delta_B = \epsilon_\Gamma^{zx(y)} - \epsilon_\Gamma^{x^2-y^2}$  (FIG. 2). The latter is due to the slightly deformed tetrahedral crystal field by the 4 Se atoms around the Fe atom. For the  $\text{KFe}_2\text{Se}_2$  systems,  $\epsilon_t$  and  $\Delta_B$  are 18 meV and 13 meV, respectively; while for the  $\text{BaFe}_2\text{As}_2$  systems, they are -297 meV and 204 meV, respectively. Similar to the  $\text{BaFe}_2\text{As}_2$  band structure, the bands close to  $E_F$  from  $\Gamma$  to  $Z$  are mostly flat, except for the one cross the Fermi level which is due to the hybridization of Fe-3d and Se-4p orbitals. It is worthy noting that the structural relaxation does not change the number of bands across the Fermi level, nor the orbital character of these bands for  $\text{KFe}_2\text{Se}_2$ , in contrast to the cases for  $\text{LaFeAsO}$  and  $\text{BaFe}_2\text{As}_2$ . However, the structural optimization expands the band splittings  $\Delta_B$  to 314 meV, and shifts the top of fully occupied d bands  $\epsilon_t$  to 149 meV.

The band structure we obtained is then fitted using the maximally localized Wannier function (MLWF) method<sup>30,31</sup> (FIG. 2) to obtain a model Hamiltonian for reconstructing the Fermi surfaces. To perform the fitting, we chose the 16 bands from  $E_F - 6.0$  eV to  $E_F + 2.0$  eV, and 16 initial guess orbitals including the Fe-3d and Se-4p to ensure the fitting quality. Nevertheless, it is possible to fit the band structure with slightly worse quality with the 10 Fe-3d orbitals only, in order to reduce the Hamiltonian size. Applying the symmetry, the number of orbitals could be further brought down to five.

We show the parent  $\text{KFe}_2\text{Se}_2$  Fermi surface in FIG. 3(a). The Fermi surface of the parent  $\text{KFe}_2\text{Se}_2$  consists of two sheets around  $M$ -point and one sheet around  $\Gamma$ .

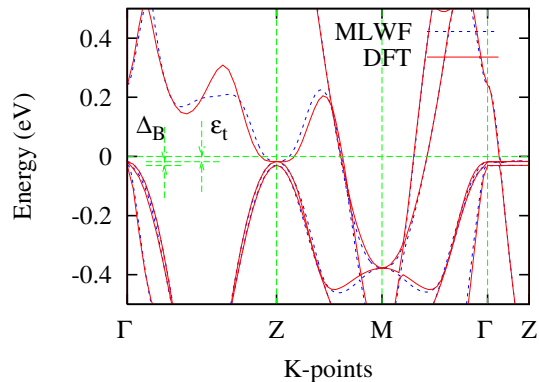
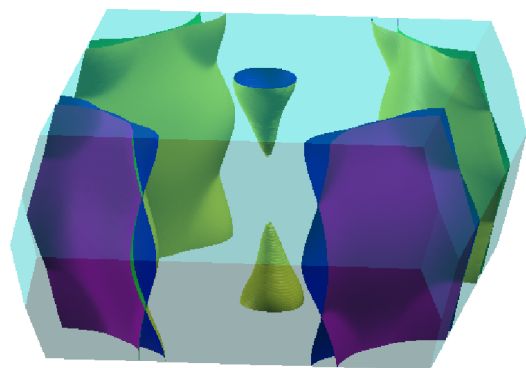


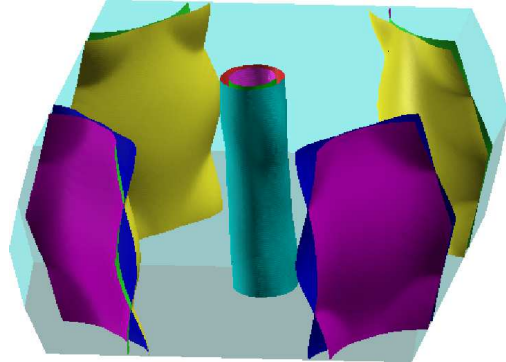
FIG. 2. Band structure of non-magnetic  $\text{KFe}_2\text{Se}_2$  calculated with the experimental structure. The solid line is the density functional theory (DFT) result and the dashed line is fitted with the maximally localized wannier function (MLWF) method.

Despite of the similarities between the  $\text{KFe}_2\text{Se}_2$  and the  $\text{BaFe}_2\text{As}_2$  systems, two distinctions are apparent. First of all, the two sheets around  $M$  points in  $\text{KFe}_2\text{Se}_2$  are much more symmetric than those in  $\text{BaFe}_2\text{As}_2$ . If we define  $k_F(\theta)$  to be the  $k$ -vector from the  $M$  point to the Fermi surface sheet, where  $\theta$  denotes the angle formed by the vector and  $M-M'$  (as shown in FIG. 3(c)), we could further define  $\eta = 1 - \frac{k_F(45^\circ)}{k_F(-45^\circ)}$ . For the two sheets around  $M$  in  $\text{KFe}_2\text{Se}_2$ , both yield  $\eta < 1\%$ , while for the  $\text{BaFe}_2\text{As}_2$  system the inner sheet has  $\eta = 48\%$  and the outer sheet has  $\eta = 41\%$ . This feature suggests that the electronic structure of  $\text{KFe}_2\text{Se}_2$  is in fact much closer to FeSe instead of  $\text{BaFe}_2\text{As}_2$ . Secondly, the sheets around  $\Gamma$  are completely different between  $\text{KFe}_2\text{Se}_2$  and  $\text{BaFe}_2\text{As}_2$  or FeSe. Three sheets were observed for  $\text{BaFe}_2\text{As}_2$  or FeSe system, which constitutes the three hole pockets for the system. For  $\text{KFe}_2\text{Se}_2$  system, only one sheet exists around  $(0,0,k_z)$  axis, which is highly 3-D and vanishes around  $\Gamma$ . Thus, the Fermi surface nesting effect is absent in the parent  $\text{KFe}_2\text{Se}_2$  compound. Nevertheless, one could achieve FeSe-like fermi surface using the rigid band model simply by shifting down the fermi level (FIG. 3(d)), or effectively by hole doping. From the band structure calculation, the Fermi level has to be shifted down by 0.2 eV in order to recover the Fermi surface nesting effect. The DOS result indicates that shifting down  $E_F$  by 0.2 eV corresponds to 1.0  $|e|$  hole doping effectively, or completely removing K from  $\text{KFe}_2\text{Se}_2$ . Due to the loss of Fermi surface nesting, the magnetism of  $\text{KFe}_2\text{Se}_2$  is not simply due to the Fermi surface nesting effect. Instead, it is possible that the localized Fe-3d orbitals plays an essential role in the magnetism. Using the same model, we could also obtain the Fermi surface for  $\text{K}_{1-x}\text{Fe}_2\text{Se}_2$  ( $x = 0.2$ ), as shown in FIG. 3(b), which could be an analogue to an electron-doped 11 system.

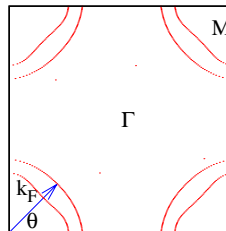
Finally, we study the  $U$ -dependence of the magnetic coupling strength  $J_1$  and  $J_2$  using the GGA+ $U$  method,



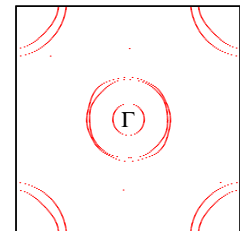
(a)  $x = 0.0$



(b)  $x = 0.2$



(c)  $x = 0.0$



(d)

FIG. 3. Fermi surface of  $\text{K}_{1-x}\text{Fe}_2\text{Se}_2$  reconstructed using the MLWFs. Panel 3(a) and 3(c) are the plots for the parent compound ( $x = 0.0$ ); panel 3(b) is the plot for  $x = 0.2$ ; panel 3(d) is obtained by shifting  $E_F$  by -0.2 eV. Panel 3(c) and 3(d) are the 2-D plots of cross-section at  $k_z = 0.0$ . Only the  $k_F$  vector of the outer sheet is drawn in Fig. 3(c) for the sake of visibility.

to test if the COL configuration remains as the ground state if there is electron correlation beyond LDA. A series of  $U$  from 1.0 eV to 6.0 eV were used to optimize the lattice constants as well as the internal coordinates for NM/CBD/COL configurations, and then  $J_1$  and  $J_2$  under different  $U$  were fitted using  $m_{\text{Fe}} = 1.0\mu_B$ . Both  $J_1$  and  $J_2$  show linear dependence with respect to the on-site energy  $U$ , and the collinear state remains the ground state within a reasonable  $U$  range.

In conclusion, we have studied the electronic structure of  $\text{KFe}_2\text{Se}_2$  using first-principles calculations. The ground state of  $\text{KFe}_2\text{Se}_2$  turns out to be collinear anti-

ferromagnetic configuration with  $2.26 \mu_B$  magnetic moment on Fe atoms, similar to  $\text{BaFe}_2\text{As}_2$ . The  $J_1$  and  $J_2$  coupling strengths are calculated to be 0.038 eV and 0.029 eV, respectively. Although the band structure is similar to heavily electron-doped  $\text{BaFe}_2\text{As}_2$ , the Fermi surface suggests that the system is much closer to an electron-doped FeSe system. The Fermi surface nesting effect is absent in the parent  $\text{KFe}_2\text{Se}_2$  compound, thus the antiferromagnetism is possibly due to the local moments instead of the itinerant electrons. Since the  $\text{KFe}_2\text{Se}_2$  is electron-doped, the superconductivity could be introduced with hole-doping or, effectively, K or Fe deficiencies.

We would like to thank Hong Ding and Gang Wang for calling our attention to the  $\text{KFe}_2\text{Se}_2$  compound reported in Ref.<sup>21</sup>. We also thank Guanghan Cao, Xiaoyong Feng, and Qimiao Si for helpful discussions. This work was supported by the NSFC, the 973 Project of the MOST and the Fundamental Research Funds for the Central Universities of China (No. 2010QNA3026). All the calculations were performed on Hangzhou Normal University College of Science High Performance Computing Center.

Note added: After submitting this work to arXiv, we became aware of two recent papers<sup>32,33</sup> where some related calculations have been also performed on the  $\text{KFe}_2\text{Se}_2$  compound.

- 
- <sup>1</sup> Y. Kamihara, T. Watanabe, M. Hirano, and H. Hosono, *J. Am. Chem. Soc.*, **130**, 3296 (2008).
- <sup>2</sup> M. Rotter, M. Tegel, and D. Johrendt, *Phys. Rev. B*, **78**, 020503 (2008).
- <sup>3</sup> M. J. Pitcher, D. R. Parker, P. Adamson, S. J. C. Herkelrath, A. T. Boothroyd, R. M. Ibberson, M. Brunelli, and S. J. Clarke, *Chem. Comm.*, **88**, 5918 (2008).
- <sup>4</sup> J. H. Tapp, Z. Tang, B. Lv, K. Sasmal, B. Lorenz, P. C. W. Chu, and A. M. Guloy, *Phys. Rev. B*, **78**, 060505(R) (2008).
- <sup>5</sup> X.-H. Chen, T. Wu, G. Wu, R.-H. Liu, H. Chen, and D.-F. Fang, *Nature*, **453**, 761 (2008).
- <sup>6</sup> G. F. Chen, Z. Li, D. Wu, G. Li, W. Z. Hu, J. Dong, P. Zheng, J. L. Luo, and N. L. Wang, *Phys. Rev. Lett.*, **100**, 247002 (2008).
- <sup>7</sup> Z.-A. Ren, G.-C. Che, X.-L. Dong, J. Yang, W. Lu, W. Yi, X.-L. Shen, Z.-C. Li, L.-L. Sun, F. Zhou, and Z.-X. Zhao, *Europhys. Lett.*, **83**, 17002 (2008).
- <sup>8</sup> H.-H. Wen, G. Mu, L. Fang, H. Yang, and X. Zhu, *Europhys. Lett.*, **82**, 17009 (2008).
- <sup>9</sup> C. Wang, L. Li, S. Chi, Z. Zhu, Z. Ren, Y. Li, Y. Wang, X. Lin, Y. Luo, S. Jiang, X. Xu, G. Cao, and Z. Xu, *Europhys. Lett.*, **83**, 67006 (2008).
- <sup>10</sup> J. Dong, H. J. Zhang, G. Xu, Z. Li, G. Li, W. Z. Hu, D. Wu, G. F. Chen, X. Dai, J. L. Luo, Z. Fang, and N. L. Wang, *Europhys. Lett.*, **83**, 27006 (2008).
- <sup>11</sup> D. J. Singh and M. H. Du, *Phys. Rev. Lett.*, **100**, 237003 (2008).
- <sup>12</sup> T. Yildirim, *Phys. Rev. Lett.*, **101**, 057010 (2008).
- <sup>13</sup> I. I. Mazin, D. J. Singh, M. D. Johannes, and M. H. Du, *Phys. Rev. Lett.*, **101**, 057003 (2008).
- <sup>14</sup> C. Cao, P. J. Hirschfeld, and H.-P. Cheng, *Phys. Rev. B*, **77**, 220506 (2008).
- <sup>15</sup> F. Ma and Z.-Y. Lu, *Phys. Rev. B*, **78**, 033111 (2008).
- <sup>16</sup> F. Ma, Z.-Y. Lu, and T. Xiang, *Phys. Rev. B*, **78**, 224517 (2008).
- <sup>17</sup> D. J. Singh, *Phys. Rev. B*, **78**, 094511 (2008).
- <sup>18</sup> Q. Si and E. Abrahams, *Phys. Rev. Lett.*, **101**, 076401 (2008).
- <sup>19</sup> D. Kasinathan, A. Ormeci, K. Koch, U. Burkhardt, W. Schnelle, A. Leithe-Jasper, and H. Rosner, *New J. Phys.*, **11**, 025023 (2009).
- <sup>20</sup> F. Rullier-Albenque, D. Colson, A. Forget, P. Thuéry, and S. Poissonnet, *Phys. Rev. B*, **81**, 224503 (2010).
- <sup>21</sup> J. Guo, S. Jin, G. Wang, S. Wang, K. Zhu, T. Zhou, M. He, and X. Chen, *Phys. Rev. B*, **82**, 180520(R) (2010).
- <sup>22</sup> P. Giannozzi, S. Baroni, N. Bonini, and *et al.*, *Journal of Physics: Condensed Matter*, **21**, 395502 (2009).
- <sup>23</sup> C. Cao, Y. ning Wu, R. Hamdan, Y.-P. Wang, and H.-P. Cheng, *New J. Phys.*, **12**, 123029 (2010).
- <sup>24</sup> H. J. Monkhorst and J. D. Pack, *Phys. Rev. B*, **13**, 5188 (1976).
- <sup>25</sup> J. P. Perdew, K. Burke, and M. Ernzerhof, *Phys. Rev. Lett.*, **77**, 3865 (1996).
- <sup>26</sup> website: <http://elk.sourceforge.net>.
- <sup>27</sup> A. Subedi, L. Zhang, D. J. Singh, and M. H. Du, *Phys. Rev. B*, **78**, 134514 (2008).
- <sup>28</sup> D. J. Singh, M. H. Du, L. Zhang, A. Subedi, and J. An, *Physica C*, **469**, 886 (2009).
- <sup>29</sup> D. J. Singh, *Physica C*, **469**, 418 (2009).
- <sup>30</sup> I. Souza, N. Marzari, and D. Vanderbilt, *Phys. Rev. B*, **65**, 035109 (2001).
- <sup>31</sup> A. A. Mostofi, J. R. Yates, Y.-S. Lee, I. Souza, D. Vanderbilt, and N. Marzari, *Comp. Phys. Comm.*, **178**, 685 (2008).
- <sup>32</sup> X.-W. Yan, M. Gao, Z.-Y. Lu, and T. Xiang, *ArXiv:1012.5536*.
- <sup>33</sup> I. Shein and A. Ivanovskii, *ArXiv:1012.5164*.